

# Increased cross-correlation in cascaded four-wave mixing processes

J. Fan and A. Migdall

*Optical Technology Division, National Institute of Standards and Technology  
100 Bureau Drive, Mail Stop 8441, Gaithersburg, MD 20899-8441  
and Joint Quantum Institute, University of Maryland, College Park, MD 20742  
[Jfan@nist.gov](mailto:Jfan@nist.gov)*

L. J. Wang

*Max-Planck Institute for Optics, Information and Photonics, & Univ. of Erlangen, 91058 Erlangen, Germany*

**Abstract:** We report the measurement of increased noise cross-correlation between stokes and anti-stokes beams created in cascaded four-wave mixing processes with dual pump wavelengths. This method may be useful in creating highly correlated twin beams for various applications including quantum information processing.

©2007 Optical Society of America

**OCIS codes:** (190.4380) Nonlinear optics, four wave mixing.

---

## References and links

1. J. E. Sharping, M. Fiorentino, A. Coker, and P. Kumar, "Four-wave mixing in microstructure fiber," *Opt. Lett.* **26**, 1048 (2001).
2. R. Rang, J. Lasri, P. Devgan, Jay E. Sharping, and P. Kumar, "Microstructure-fiber-based optical parametric amplifier with gain slope of 200 dB/W/km in the telecom range," *Electron. Lett.* **39**, 195 (2003).
3. J. D. Harvey, R. Leonhardt, S. Coen, G. K. L. Wong, J. C. Knight, W. J. Wadsworth, and P. St. J. Russel, "Scalar modulation instability in the normal dispersion regime by use of a photonic crystal fiber," *Opt. Lett.* **28**, 2225 (2003).
4. S. Radic, C. J. McKinstrie, R. M. Jopson, J. C. Centanni, Q. Lin and G. P. Agrawal, "Record performance of parametric amplifier constructed with highly nonlinear fiber," *Electron. Lett.* **39**, 838 (2003).
5. K. Inoue, "Polarization effect on four-wave mixing efficiency in a single-mode fiber," *IEEE J. Quantum Electron.* **28**, 883 (1992).
6. J. H. Lee, Z. Yusoff, W. Belardi, M. Ibsen, T. M. Monro and D. J. Richardson, "A tunable WDM wavelength converter based on cross-phase modulation effects in normal dispersion holey fiber," *IEEE Photon. Technol. Lett.* **15**, 437 (2003).
7. Y. Wang, C. Yu, T. Luo, L. Yan, Z. Pan, and A. E. Willner, "Tunable all-optical wavelength conversion and wavelength multicasting using orthogonally polarized fiber FWM," *J. Lightwave Technol.* **23**, 3331 (2005).
8. J. E. Sharping, M. Fiorentino, P. Kumar, and R. S. Windeler, "Optical parametric oscillator based on four-wave mixing in microstructure fiber," *Opt. Lett.* **27**, 1675 (2002).
9. C. J. S. De Matos, J. R. Taylor, K. P. Hansen, "Continuous-wave, totally fiber integrated optical parametric oscillator using holey fiber," *Opt. Lett.* **29**, 983 (2004).
10. Y. Deng, Q. Lin, F. Liu, G. P. Agrawal, and W. H. Know, "Broadly tunable femtosecond parametric oscillator using a photonic crystal fiber," *Opt. Lett.* **30**, 1234 (2005).
11. J. Ye and S. T. Cundiff: *Femtosecond Optical Frequency Comb: Principle, Operation and Applications*, (Springer, 2005).
12. C. J. McKinstrie and M. G. Raymer, "Four-wave-mixing cascades near the zero-dispersion frequency," *Opt. Express* **14**, 9600-9610 (2006)  
<http://www.opticsinfobase.org/abstract.cfm?URI=oe-14-21-9600>
13. C. J. McKinstrie, S. Radic, M. G. Raymer, and L. Schenato, "Unimpaired phase-sensitive amplification by vector four-wave mixing near the zero-dispersion frequency," *Opt. Express* **15**, 2178-2189 (2007)  
<http://www.opticsinfobase.org/abstract.cfm?URI=oe-15-5-2178>
14. C. M. Caves, and B. L. Schumaker, "New formalism for two-photon quantum optics. I. Quadrature phases and squeezed states", *Phys. Rev. A*, 31 3068(1985).

15. X. Li, P. Voss, Jay E. Sharping, J. Chen, P. Kumar, "Optical-fiber source of polarization-entangled photon pairs in the 1550 nm telecom band," *Phys. Rev. Lett.* **94**, 053601 (2005).
16. J. Fan, A. Dogariu, L. J. Wang, "Generation of correlated photon pairs in a microstructure fiber," *Opt. Lett.* **30**, 1530 (2005).
17. J. Fan, A. Migdall, and L. J. Wang, "Efficient generation of correlated photon pairs in a microstructure fiber," *Opt. Lett.*, **30**, 3368 (2005).
18. Jay E. Sharping, M. Fiorentino, and P. Kumar, "Observation of twin-beam-type quantum correlation in optical fiber," *Opt. Lett.* **26**, 367 (2001).
19. J. Fan, A. Dogariu, L. J. Wang, "Parametric amplification in a microstructure fiber," *Appl. Phys. B* **81**, 801(2005).
20. J. Fan, A. Migdall, "Generation of cross-polarized photon pairs in a microstructure fiber with frequency-conjugate laser pump pulses," *Opt. Express* **13**, 5777-5782 (2005)  
<http://www.opticsinfobase.org/abstract.cfm?URI=oe-13-15-5777>
21. J. Chen, K. F. Lee, C. Liang, and P. Kumar, "Fiber-based telecom-band degenerate-frequency source of entangled photon pairs," *Opt. Lett.* **31**, 2798 (2006).
22. Corning part # 2110-03, <http://www.corning.com/>
23. G. P. Agrawal: *Nonlinear Fiber Optics*, 2<sup>nd</sup> ed. (New York: Academic 1995).
24. X. Y. Zou, L. J. Wang, and L. Mandel, "Violation of classical probability in parametric down-conversion," *Optics Comm.* **84**, 351 (1991).
25. L. J. Wang, C. K. Hong, and S. R. Friberg, "Generation of correlated photons via four-wave mixing in optical fibers," *J. Opt. B: Quantum Semiclass. Opt.* **3**, 346 (2001).
26. C. J. McKinstrie, S. Radic, and A. R. Chraplyvy, "Parametric amplifiers driven by two pump waves," *IEEE J. Sel. Top. Quantum Electron.* **8**, 538(2002).
27. C. J. McKinstrie, S. Radic, and M. G. Raymer, "Quantum noise properties of parametric amplifiers driven by two pump waves," *Opt. Express* **12**, 5037-5066 (2004)  
<http://www.opticsinfobase.org/abstract.cfm?URI=oe-12-21-5037>

## 1. Introduction

Four-wave mixing (FWM) has been used in many optical communication applications such as parametric amplification [1-4], wavelength conversion [5-7], and parametric oscillation [8-10]. It is also used to create super-continuum light and frequency combs for applications in spectroscopy and absolute frequency calibration [11]. Recently there has been a growing interest in studying the FWM with multiple pump wavelengths [12, 13]. In most experiments reported so far with two pump wavelengths  $\omega_{p1} < \omega_{p2}$ , the two stimulated degenerate FWM processes  $2\omega_{p1} = \omega_{st} + \omega_{p2}$  and  $2\omega_{p2} = \omega_{p1} + \omega_{as}$  dominate over the spontaneous non-degenerate FWM process  $\omega_{p1} + \omega_{p2} = \omega_{st} + \omega_{as}$  in creating stokes ( $\omega_{st}$ ) and anti-stokes ( $\omega_{as}$ ) light in the spectral side bands. Study of cross-correlation between the created stokes and anti-stokes light is of special interest for the generation of squeezed states [14] or correlated photon pairs [15-17] that may be of use for high resolution imaging or quantum information applications. While there has been consistent interest in studying the correlation between the stokes and anti-stokes light created in a degenerate FWM process with a single pump wavelength [18, 19], correlation studies have not been made of FWM with multiple pump wavelengths because it was assumed there is no direct correlation between the stokes and anti-stokes beams due to the dominance of degenerate FWM amplification.

Recently it was shown [12, 16, 20] that when fiber dispersion varies slowly near the zero-dispersion wavelength ( $\lambda_{ZDW}$ ), phase-matching or quasi-phase-matching can be satisfied between the pump, signal and idler fields. By arranging a pair of pump beams with frequencies ( $\omega_{st}$ ,  $\omega_{as}$ ) conjugate with respect to  $\lambda_{ZDW}$ , such a process can occur and dominate with  $\omega_{st} + \omega_{as} = 2\omega_{ZDW}$ . The frequency-degenerate two-photon light was produced efficiently with this method in the visible and the near infrared [16, 20, 21].

When light is created at the middle frequency in the two-photon state by spontaneous non-degenerate FWM instead of in single-photon state via stimulated degenerate FWM, this contradicts the accepted view as described above. One may further consider that this dominance of spontaneous non-degenerate FWM relative to stimulated degenerate FWM might also appear in the creation of stokes and anti-stokes wavelengths in the spectral side

bands,  $\omega_{p1} + \omega_{p2} \rightarrow \omega_{st} + \omega_{as}$ , which also contradicts the conventional wisdom. The Stokes and anti-Stokes wavelengths created by this spontaneous non-degenerate FWM process exhibit inherent correlation. In this paper we report what we believe is the first measurement of the cross-correlation between frequency-matched Stokes and anti-Stokes wavelengths created in a FWM process with dual-pump wavelengths. As the FWM process cascades to higher order, the higher order Stokes and anti-Stokes wavelengths show increased cross-correlation.

## 2. Experiment and discussion

The experiment (Fig. 1) begins with a 3 ps linearly polarized laser pulse ( $\lambda_p = 834.9$  nm) coupled into a microstructure fiber\* [22] MF<sub>1</sub> ( $\gamma = 70$  W/km, dispersion  $D = 1.8$  ps/nm/km at  $\lambda_p = 835$  nm) along one principal axis to generate quasi-super-continuum light at a repetition rate of 80 MHz, from which we select a pair of wavelengths (Stokes,  $\lambda_{st} = 836.9$  nm and anti-Stokes,  $\lambda_{as} = 832.6$  nm). Using a two-pass grating configuration, the two selected light pulses are put back in the same single spatial-mode and then coupled into a second microstructure fiber, MF<sub>2</sub> along the same principal axis used for MF<sub>1</sub>. (MF<sub>1</sub> and MF<sub>2</sub> are two identical fibers with MF<sub>1</sub> to be 1.8 m and MF<sub>2</sub> to be 1 m.) The delay between the two pulses is adjusted to maximize the power of the third-order anti-Stokes light out of MF<sub>2</sub> (Fig. 1 inset). The light output from MF<sub>2</sub> is directed to a second grating to separate the wavelengths.

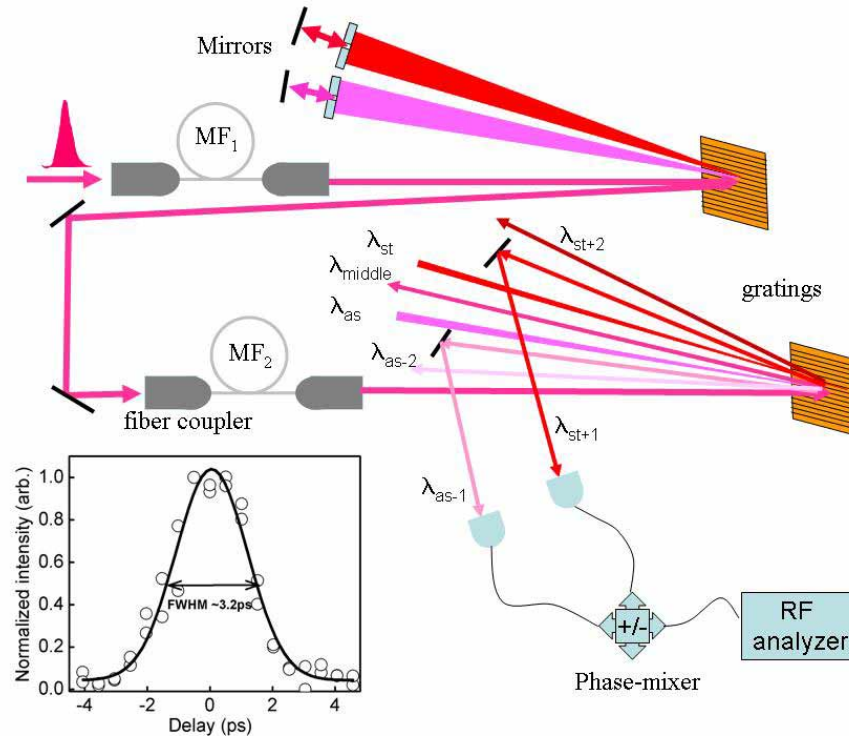


Fig. 1. Setup for FWM in two MFs. Inset- Third-order anti-Stokes output ( $\lambda_{as-3} = 818.7$  nm) of MF<sub>2</sub> versus delay between the two inputs into MF<sub>2</sub>.

A spectrum of the light exiting MF<sub>2</sub> is shown in Fig. 2(a), where the two pump wavelengths ( $\lambda_{st}$  and  $\lambda_{as}$ ) are labeled, along with wavelengths  $\lambda_{st+1} = 841.9$  nm and  $\lambda_{as-1} =$

\* Certain trade names and company products are mentioned in the text or identified in an illustration in order to specify adequately the experimental procedure and equipment used. In no case does such identification imply recommendation or endorsement by the National Institute of Standards and Technology, nor does it imply that the products are necessarily the best available for the purpose.

828.1 nm,  $\lambda_{st+2} = 846.7$  nm and  $\lambda_{as-2} = 823.4$  nm, and  $\lambda_{st+3} = 851.6$  nm and  $\lambda_{as-3} = 818.7$  nm designating the first, second, and third order stokes and anti-stokes wavelengths, respectively. It is easy to verify energy conservation with,

$$\begin{aligned} \omega_{as} + \omega_{st} &= \omega_{as-1} + \omega_{st+1} \\ &= \omega_{as-2} + \omega_{st+2} \\ &= \omega_{as-3} + \omega_{st+3} \\ &= 2\omega_p = 4.51 \times 10^3 \text{ THz}. \end{aligned} \quad (1)$$

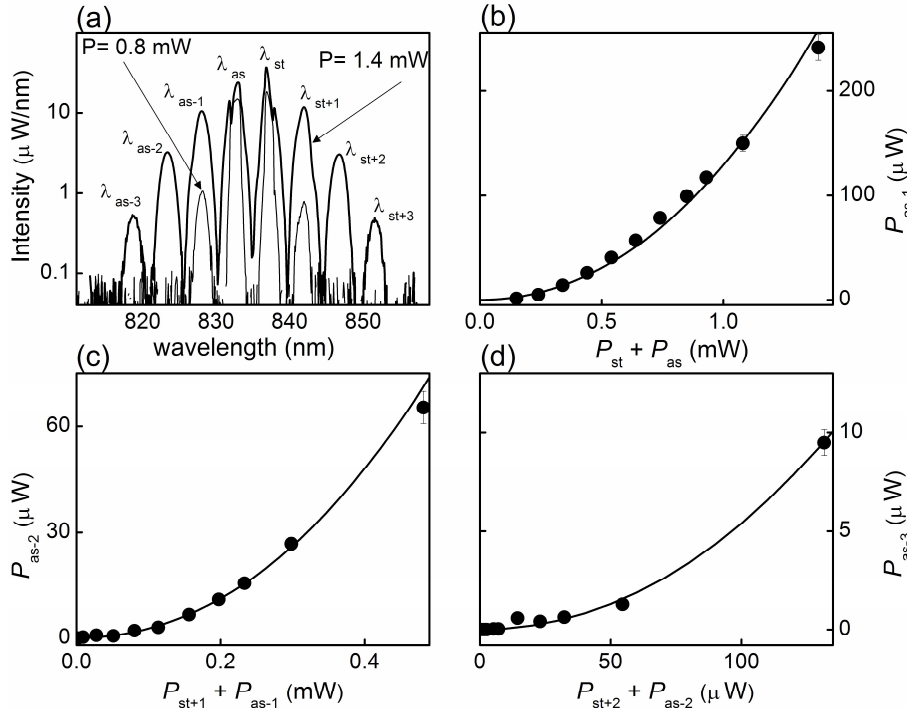


Fig. 2. (a) Spectral output of MF<sub>2</sub> at two input powers  $P_{st} + P_{as} = 1.4$  mW (thick line) and 0.8 mW (thin line). (b), (c) and (d)  $P_{as-i}$  average output anti-Stokes power of order  $i = 1, 2, 3$ , versus  $P_{as-(i-1)} + P_{st+(i-1)}$ , the sum of the average powers of the preceding FWM order. The data set (dots) is fit with Eq. (2) times a scale factor (line).

For each order, we plot the average power of the anti-Stokes light as a function of the total average power of the preceding order stokes and anti-stokes wavelengths in Figs. 2(b)-(d). Each curve shows an exponentially increasing power-dependence, where if we assume that the non-degenerate FWM dominates over other nonlinear processes in the generation of each order Stokes and anti-Stokes wavelength, and we assume that the pump power is not significantly consumed, the gain for each order FWM process is [23]

$$G = \left(1 + \frac{\kappa^2}{4g^2}\right) \sinh^2(gz), \quad (2)$$

where  $\kappa = \beta_2(\Delta\omega)^2 + \gamma(P_{st,i} + P_{as,i})$  accounts for the FWM phase matching, and  $g = [(\gamma(P_{st,i} + P_{as,i}))^2 - (\frac{\kappa}{2})^2]^{1/2}$  is the FWM gain,  $P_{st,i}$  and  $P_{as,i}$  are the powers of the parent stokes and anti-stokes pump light with  $i = 0, 1, 2$  representing the order of the FWM process,

$\beta_2 = -\frac{\lambda_0^2}{2\pi c} D$  is the group velocity dispersion and  $z$  is fiber length. As seen in Figs. 2(b)-2(d), the data are consistent with the exponential behavior of Eq. (2).

The Stokes and anti-Stokes light separated by the grating are each individually coupled into a fast photo-diode. To measure the correlation between conjugate wavelengths given by energy conservation (Eq. (1)), the induced photo-currents,  $I_{st+i}$  and  $I_{as-i}$  are fed into a phase-mixer to create sum- and difference- currents  $I_+$  and  $I_-$ , which are measured by a RF spectrum analyzer [19]. The difference noise current density for perfect correlation is  $\langle I_-^2 \rangle = 0$  while for two completely uncorrelated wavelengths  $\langle I_-^2 \rangle = \langle I_+^2 \rangle$ , assuming equal detection efficiencies. A ratio  $\Gamma = \frac{\langle I_+^2 \rangle - \langle I_-^2 \rangle}{\langle I_+^2 \rangle + \langle I_-^2 \rangle}$  characterizes the noise cross-correlation between the two wavelengths. For equal detection efficiencies, and perfect correlation between the two wavelengths,  $\Gamma$  approaches unity.

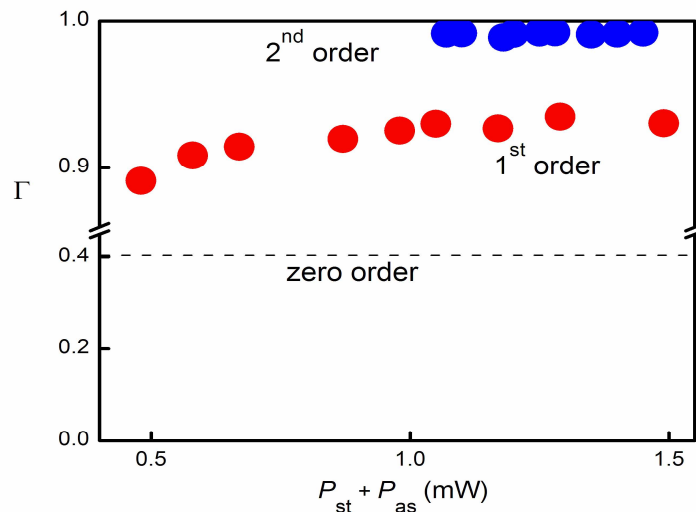


Fig. 3. Cross-correlation measurements for the twin lights generated in first and second order FWM processes in MF<sub>2</sub>. The dashed line shows cross-correlation between the two inputs to MF<sub>2</sub> for comparison.

The measured noise cross-correlations (Fig. 3) show that the two second-order wavelengths ( $\lambda_{as-2}$  and  $\lambda_{st+2}$ ) have higher cross-correlation than the two first-order wavelengths ( $\lambda_{as-1}$  and  $\lambda_{st+1}$ ). The correlation increases with power and saturates at high power, where the difference-noise falls below the sum-noise by 14 dB for the first order, and 24 dB for the second order. We recall that the two frequency-conjugate inputs to MF<sub>2</sub> were selected from the spontaneous degenerate FWM output of MF<sub>1</sub>, where the difference-noise falls below the sum-noise by 3.6 dB. (The light coupling-out efficiency from MF<sub>2</sub> is 80%, the grating efficiency is 90% and the detector efficiency is 80%.) This is close to the maximum noise correlation of 5 dB measured in a previous degenerate FWM experiment with a single pump wavelength [18]; while in our experiment the subsequent cascaded FWM in MF<sub>2</sub> creates twin wavelengths with much higher cross-correlations. Considering that the two FWM processes in MF<sub>1</sub> and MF<sub>2</sub> are inherently cascaded, a 10 dB increase (difference-noise falling below the sum-noise) is obtained for each higher order cascaded process. (The cross-correlation between the third- and higher-order Stokes and anti-Stokes wavelengths could not be resolved due to limited detection sensitivity.)

It is known that purely classical noise sources can also result in  $\langle I_-^2 \rangle = 0$  and  $\Gamma = 1$ . A number of approaches can be used to differentiate between classical and non-classical effects. One way is to compare the difference-noise with the shot noise limit [18], another way is to examine the violation of classical probability [24]. For our experiment, we used yet another method to examine the non-classicality. We varied the wavelengths of one of the two inputs to MF<sub>2</sub>, and observed the wavelengths of the created spectral side bands shifting correspondingly. We saw the measured sum-noise remain nearly constant, while the difference-noise rose to the level of the sum-noise. This decreased correlation shows that the spontaneous non-degenerate FWM process is replaced by the stimulated degenerate FWM process in MF<sub>2</sub> as we vary the wavelength. In our previous publication [25], we discussed how the spontaneous FWM process is a quantum process. Hence, the noise correlation measurement, together with the gain measurement, strongly suggests that spontaneous non-degenerate FWM also dominates in the cascaded process in creating the stokes and anti-stokes wavelengths, as well as dominating the creation of two-photon light at the middle frequency. When repeating the same type of experiment with a different microstructure fiber which has similar nonlinear gain but different dispersion properties, we did not observe correlation between those two wavelengths in the side spectral bands, suggesting that dispersion plays an important role. It is known that for a dual-pump wavelength process in an optical fiber, several third-order nonlinear processes such as degenerate FWM, non-degenerate FWM, and Bragg scattering can occur, each with different phase-matching conditions [26, 27]. In practice there can be significant interactions between these processes via their phase-matching conditions. With appropriate dispersion management, one nonlinear process can be enhanced while other processes are relatively suppressed. In our experiment, by arranging to have the non-degenerate FWM dominate at the middle frequency, we observe its dominance in creating the higher order side spectral bands as well.

In conclusion, we have measured, for the first time, increased classical cross-correlation for high order wavelength-matched stokes and anti-stokes light created from a cascaded FWM process, suggesting the dominance of spontaneous non-degenerate FWM in the interaction. The demonstrated correlation feature may have potential for producing highly correlated twin beams, and correlated two-photon light. This correlation feature depends on the fiber dispersion, as evidenced by our tests with different fibers and the variation of pump wavelength in the experiment. Theoretical work is needed to understand the fundamental physics that generates this correlation feature, to guide our future experimental studies. This analysis is under way.

### **Acknowledgments**

This work was supported in part by the MURI Center for Photonic Quantum Information Systems (ARO/DTO program DAAD19-03-1-0199) and the DTO entangled source programs. LJW thanks the support of JST (CREST).